AD-A121 726 ANALYSIS OF SENSORY EVOKED POTENTIALS USING NORMALIZED CROSS-CORRELATION.. (U) NAVAL BIODYNAMICS LAB NEW ORLEANS LA M D BERGER JUL 82 NBDL-8L1R003 1/1

UNCLASSIFIED F/G 6/19 NL

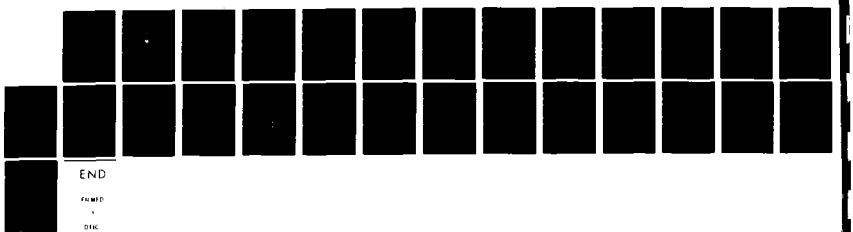

END

FILMED

DTIC

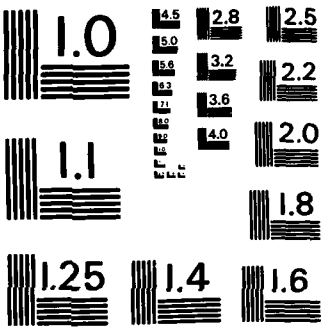

NBDL -82R015

ANALYSIS OF SENSORY EVOKED POTENTIALS USING NORMALIZED CROSS-CORRELATION FUNCTIONS AND POLYEXPONENTIAL REGRESSION

Michael D. Berger, Ph.D.

July 1982

NAVAL BIODYNAMICS LABORATORY
New Orleans, Louisiana

Approved for public release. Distribution unlimited.

REPORT DOCUMENTATION PAGE

READ INSTRUCTIONS BEFORE COMPLETING FORM

1. REPORT NUMBER: NBDL-82015
2. GOVT ACCESSION NO.: AD-A121726
3. RECIPIENT'S CATALOG NUMBER:

4. TITLE (and Subtitle): Analysis of Sensory Evoked Potentials Using Normalized Cross-Correlation Functions and Polyexponential Regression

5. TYPE OF REPORT & PERIOD COVERED: Research Report

6. PERFORMING ORG. REPORT NUMBER: NBDL-81R003

7. AUTHOR(s): Michael D. Berger, Ph.D.

8. CONTRACT OR GRANT NUMBER(s):

9. PERFORMING ORGANIZATION NAME AND ADDRESS:
Naval Biodynamics Laboratory
P.O. Box 29407
New Orleans, LA 70189

10. PROGRAM ELEMENT, PROJECT, TASK AREA & WORK UNIT NUMBERS: M0097-PN.001-5004

11. CONTROLLING OFFICE NAME AND ADDRESS:
Naval Medical Research and Development Command
Bethesda, MD 20014

12. REPORT DATE: July, 1982

13. NUMBER OF PAGES: 23

14. MONITORING AGENCY NAME & ADDRESS(if different from Controlling Office):

15. SECURITY CLASS. (of this report): Unclassified

15a. DECLASSIFICATION/DOWNGRADING SCHEDULE:

16. DISTRIBUTION STATEMENT (of this Report)

Approved for public release, distribution unlimited.

17. DISTRIBUTION STATEMENT (of the abstract entered in Block 20, if different from Report)

18. SUPPLEMENTARY NOTES

19. KEY WORDS (Continue on reverse side if necessary and identify by block number)

evoked potential, correlation, exponential regression, concussion, acceleration, impact, neurophysiology

20. ABSTRACT (Continue on reverse side if necessary and identify by block number)

Somatosensory evoked potentials (EPs) produced by stimulation of the dorsal columns were recorded from the cervico-medullary junction of adult Rhesus, and were analysed using normalized cross-correlation functions (NCCFs), simple peak-detection, and RMS amplitude measurement. The NCCF provided measures of latency shift and waveshape change, while the more traditional peak-detection method provided measures of peak latency and peak amplitude. The results of these procedures were plotted as functions of time relative to a single, brief experimental manipulation (impact acceleration of the whole body). Analysis by

BLOCK 20 CONTINUATION

means of the NCCF was found to be a versatile and effective technique, the advantages of which include: (1) measurement of latency shifts with little contamination by moderate changes in waveshape, (2) quantification of subtle waveshape changes, and (3) usefulness under a wide variety of noise conditions. Polyexponential regression analyses were performed on selected plots and were found to be an effective means of reducing of these data.

NBDL-82R015

ANALYSIS OF SENSORY EVOKED POTENTIALS USING NORMALIZED CROSS-CORRELATION FUNCTIONS AND POLYEXPONENTIAL REGRESSION

Michael D. Berger, Ph.D.

July 1982

Bureau of Medicine and Surgery
Work Unit M0097-PN.001-5004

Approved by

Channing L. Ewing, M.D.
Chief Scientist

Released by

Captain L. E. Williams MC USN
Commanding Officer

Naval Biodynamics Laboratory
Box 29407
New Orleans, LA. 70189

SUMMARY PAGE

THE PROBLEM

In order to evaluate impact protection devices, an impact injury model for restrained humans in a crash environment must be developed. Disruption of the functioning of the central nervous system (CNS) is an important consequence on impact injury involving the head and neck, and is an important consideration in the development of a useful impact-injury model. Ultimately, neurophysiological criteria are desired. Evoked potentials (EPs) are likely to provide appropriate neurophysiological information, but quantitative analysis of EP data presents considerable difficulty. The main purpose of the work reported here is to develop and test appropriate EP data analysis techniques. In particular, the normalized cross-correlation function (NCCF) and polyexponential regression were evaluated in this application.

FINDINGS

Data were obtained from a single experiment which is part of an on-going program to test the neurophysiological effects of indirect or inertial head-neck acceleration. An unanesthatized Rhesus monkey, with torso restrained in a seated position, and with head and neck free to move, was subjected to a peak acceleration of 963 m/s^2 in the -X direction. Recordings of somatosensory evoked potentials were obtained using recording electrodes over the cervico-medullary junction. Electrical stimuli with a duration of 0.2 ms and a current of 0.75 ma were delivered at a rate of 5 Hz to the dorsal columns at L1-L2. EPs were recorded prior to impact, through impact, and subsequent to impact. NCCFs were computed between "reference waves" which were selected portions of average evoked potentials (AEPs) computed from large segments of pre-impact data, and "test waves" which were AEPs computed from numerous small segments of pre- and post-impact data. From the NCCFs, measurements of latency shift and change in waveshape were determined, and plotted as a function of time relative to impact. Polyexponential regression was applied to some of these plots. Conventional latency and amplitude measurement techniques were also tested. The effects of varying the parameters of NCCF computation were examined. It was found that the NCCF was a powerful and flexible tool for analysis of AEP data. Polyexponential regression was found to be useful in describing the time course of the effects induced by impact.

RECOMMENDATIONS

The NCCF is powerful and effective as it stands, but other techniques, including conventional latency and amplitude measurement should also be used. The NCCF computation requires four parameters. Efficiency would be enhanced if automated algorithms to determine these parameters were developed. Polyexponential regression presents concise results, but under some conditons, its computation presents technical problems. These problems should be subject to further investigation, and also, alternative procedures should be considered.

ACKNOWLEDGEMENTS

This research was sponsored by the Naval Medical Research and Development Command and the Biophysics Program of the Office of Naval Research, and was performed under Navy work unit No. M0097-PN.001-5004. A project as complex as the one discussed here would not be possible without the dedicated cooperation of a large number of skilled people. The following list is incomplete, and is in no particular order. From the Naval Biodynamics Laboratory: Mr. L. Lustick provided valuable discussion on the mathematical procedures; Mr. G. Williamson provided administrative services in expediting computer operations; Mr. W. Anderson designed and programmed the hardware and software required for the specialized digitization procedures; Dr. E. Jessop, with the assistance of the NBDL veterinary staff, provided excellent clinical maintainence and evaluation of the subjects, as well as supervision of the electrode implantation procedures and associated logistics; Mr. A. Prell provided excellent photographic and artistic services; Mr. S. Morrill maintained and operated the physiological data aquisition system; Dr. D. Thomas provided overall project coordination, and valuable contributions to the experimental design; Dr. C. Ewing provided leadership and direction without which this work never would have been done. From the Medical College of Wisconsin: Dr. P. Walsh performed the neurosurgery; Dr. J. Myklebust performed the electrophysiological aspects of the electrode implantation. From the Texas Research Institute for Mental Science: Dr. B. Saltzberg and Mr. W. Burton supplied the CSTRIP program and some material on non-linear regression, as well as valuable discussion. From the Slidell Computer Complex, numerous staff members provided valuable assistance in dealing with the administrative and technical problems involved in inter-machine communication and analysis of a huge amount of data. In this regard, special thanks are due to Mr. F. Lovato and Mr. C. Johnson.

ANIMAL CARE

The animals used in this study were handled in accordance with the Guide for the Care of Laboratory Animals, prepared by the Committee on Care and Use of Laboratory Animals of the Institute of Laboratory Animal Resources, National Research Council.

TRADE NAMES

Trade names of materials or products of non-government organizations are cited where essential for precision in describing research procedures or evaluation of results. Their use does not constitute official endorsement or approval of the use of such commercial hardware or software.

INTRODUCTION

It is often necessary to describe concisely evoked potential (EP) data as a function of time over the course of an experiment. For this purpose, it is necessary to represent the properties of each EP by a small number of scalar measures. In most modern analytic procedures, each EP is represented by a vector in a space of high dimensionality, and the analytic problem may be described as that of reducing the dimensionality of the vector space to a small number without loss of relevent information. Because of the complex and varied nature of EP waveforms, there is no known means to affect such a reduction in dimensionaltiy that is generally applicable. It is agreed, however, that relatively few dimensions are required for an adequate representation in most cases (see Glaser and Ruchkin, 1976; Squires, et al., 1977; Squires and Donchin, 1976). In this paper, the author demonstrates the use of normalized cross-correlation functions (NCCFs) to extract two scalar measures from EPs: (1) a measure of latency shift; and (2) a measure of change in waveshape. The NCCF procedure does not provide a measure of EP amplitude. Two other procedures are also shown: a simple peak-detecting algorithm which provides measurement of peak latency and peak amplitude; and an RMS procedure which provides a measure of shape-independent amplitude over an interval. It was found that in the data examined, some of the measures appeared to decay exponentially after changes were produced by a single experimental manipulation, and the use of polyexponential regression for the analysis of such data is demonstrated.

There is no standardized procedure for latency measurement in EP work. This is in part because EPs are extended in time and vary in shape. It is therefore not possible to specify a landmark on the EP which has a constant relationship to other parts of the EP, and latency must be defined in terms of a particular procedure. The NCCF allows definition of an overall latency shift of a waveform, as well as latency shift of separate portions of the wave. Furthermore, under certain conditions, the NCCF provides latency shift information that may be more readily interpreted in terms of physiological changes than many peak-detecting procedures. Waveshape measurement is even less well defined than latency measurement. Using the NCCF it becomes possible to define waveshape change in a way that allows examination of subtle EP changes that are otherwise difficult to detect and quantify.

METHODS

The present data were taken from a single experiment which is part of a large project in progress at the Naval Biodynamics Laboratory in New Orleans. In this project, the effects of impact acceleration on human and sub-human primates are evaluated. The experiments are conducted on a horizontal accelerator which consists of a sled which decelerates gradually (0.2g) on a 213 metre track, after impact acceleration by a large horizontal piston (one metre stroke). The experiment used in this report was conducted on 14 July 1978 on Rhesus AR0761 and is referred to as run LX3010. The subject

was restrained in a nylon suit which covered the entire body except for the head and neck, and was seated in a fiberglass chair which was molded to match the shape of his back. Straps sewn to the suit firmly restrained the subject in the chair. The peak sled acceleration was approximately 963 m/s^2 in the -X direction (Thomas, et al., 1974, 1975; the back of the subject faced the direction of motion). Under these conditions of restraint and direction, 963 m/s^2 is a severe, but generally non-lethal impact for Rhesus.

Constant current, 0.75 ma., 0.2 ms., monophasic pulses were delivered to the dorsum of the spinal cord at level L1 through chronically implanted bipolar electrodes at the rate of 5 Hz. The stimulus level was the highest that was consistant with apparent comfort of the subject. Large but not maximal EP amplitudes were obtained. The EP data presented here were recorded from electrodes placed subdurally over the dorsal cervico-medullary junction (see Walsh, et al., 1978 for surgical details). The system bandpass was 30 Hz. to 1500 Hz. (-3 dB).

Evoked potential data were collected continually for an 80 minute period starting 30 minutes before impact. The data were amplified on the sled, telemetred to nearby equipment and recorded on FM tape. The data were digitized off-line on a hybrid EAI® computer at a 100 kHz. sampling rate. A software-hardware design was used which synchronized digitization with the stimuli, and minimized the numerous timing errors associated with such procedures. The digitized data were processed on a *UNIVAC 1100® series computer.*

Before further analysis, two types of average evoked potentials (AEPs) were computed: test and baseline. Numerous test AEPs were computed by counting forward and backward in time from the impact, and dividing the sequence of EPs into sub-sequences of 1, 10, or 50 EPs. A test AEP was computed from all or most of the EPs from each sub-sequence. Occasional EPs were dropped for technical reasons. Since the inter-stimulus interval was 0.2 sec., the sub-sequences covered the intervals 0.2, 2.0, and 10.0 sec. respectively. A single baseline AEP was computed from all of the EPs used to compute the pre-impact test AEPs.

Computation of an NCCF may be thought of as a search for a selected portion of the baseline AEP in each of the test waves. This selected portion is called the reference wave and was selected by specifying two latency limits. For example, the portion of the baseline AEP between 3.00 ms and 6.80 ms post-stimulus was one of the selections. To compute the NCCF, the reference wave was shifted along the test wave and Pearson's correlation coefficient was computed between the reference and test waves at each value of the shift. The NCCF is the correlation coefficient as a function of the amount of shift. To obtain the scalar measures that could be plotted as a function of time in relation to impact, each NCCF was scanned for the highest value of the correlation coefficient. This highest correlation coefficient, and the associated latency shift (of reference wave with respect to test wave) were the two scalar measures. If the maximum correlation coefficient occurred at either

end of the range of latency shifts, the corresponding data were discarded.

Two methods other than the NCCF procedure were employed: simple peak-detection and RMS amplitude measurement. In simple peak-detection, the absolute minimum or maximum within a selected latency interval was determined. The result was discarded if the absolute extremum was at the beginning or end of the selected interval. A mean amplitude computed from pre-stimulus data was then subtracted from the amplitude at the extremum. Two scalar measures, amplitude and latency, were returned for each peak-detection. In RMS amplitude measurement, first the mean amplitude in a selected latency interval of the AEP was subtracted from the AEP, and then the RMS amplitude of the residual was estimated. This resulted in a single scalar measure representing a shape-independent amplitude over the selected interval.

In selected cases, post-impact sequences of scalar measures were fitted to the equation:

$$y = \sum_{i=1}^{N} a_i \exp(b_i t) \qquad [1]$$

where a_i are exponential amplitudes, b_i are inverse time coefficients, and N is the number of exponential terms. Only real values of a_i and b_i were considered, and the values of N used were 1, 2, and 3. The method employed was a modification of the modified Gauss-Newton, least-squares method recommended by Metzler, et al. (1976, pp. 3-9). Standard errors for the regression coefficients were obtained from the diagonal terms of the estimated coefficient covariance matrix (Metzler, et al., 1976, p. 8). Initial estimates of the exponential coefficients were obtained with a modified version of the program CSTRIP (Sedman and Wagner, 1976). The pre-impact median was taken as zero for the regression analysis.

RESULTS

Appearance of Normalized Cross-Correlation Functions

Figure 1 shows sixteen NCCFs obtained by applying four reference waves to four test waves. Each reference wave was a different but sometimes overlapping portion of the same baseline AEP, (N=584, which corresponds to all pre-impact data displayed in figures 2, 3, and 4). The four reference waves are described in table 1. Three peaks are discussed throughout the following material. These are labeled a, b, and c in figure 1 and other figures. Each test wave was an AEP (N=10) taken from a different part of the experiment. The four test waves are described in table 2.

All four of the NCCFs for the pre-impact test wave (figure 1,

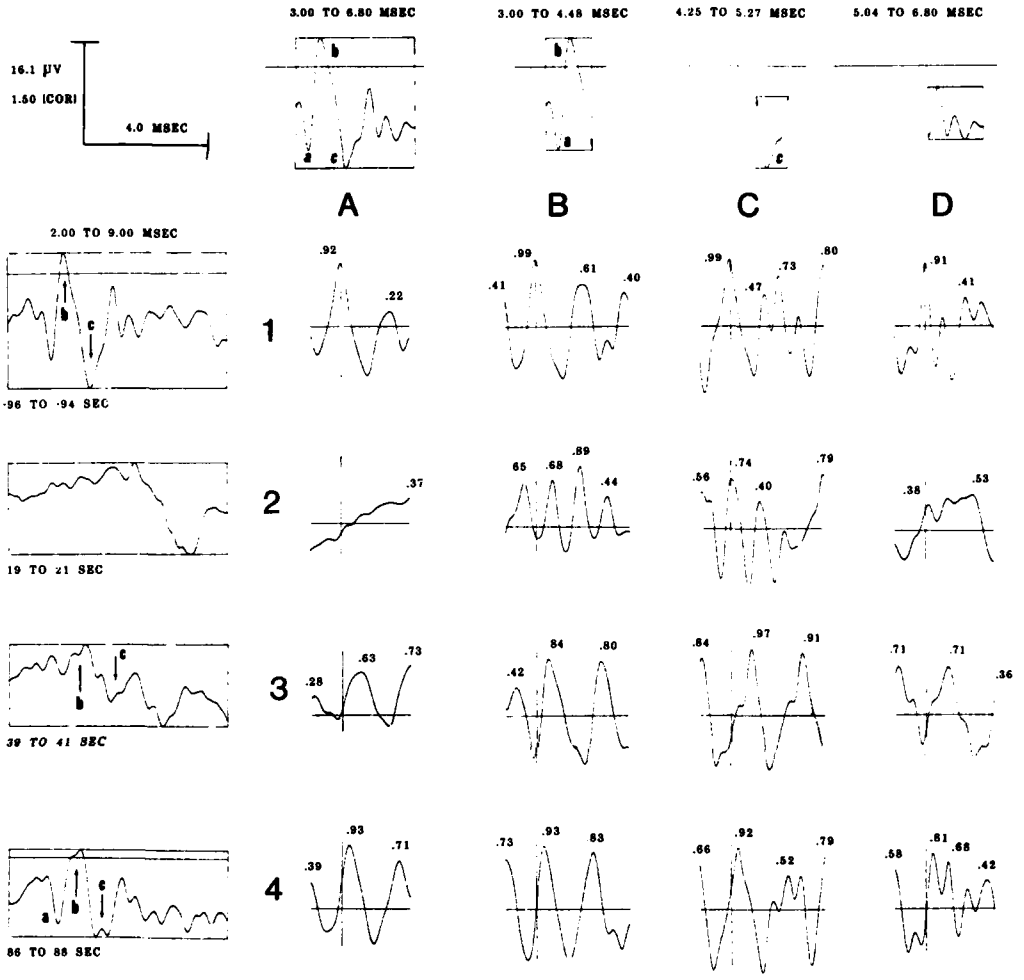

FIGURE 1

16 NCCFs (in a matrix) obtained by applying four reference waves (A-D, N=584) to four test waves (1-4, N=10). Times (in ms) above the reference waves are the selected latency limits determining the reference waves. Times (in sec) below the test waves are the stimulus time limits (relative to impact) for the AEPs constituting the test waves. Reference waves B, C and D are sub-portions of reference wave A. The latency shift range for the NCCFs in columns A and D is -1.0 to +2.2 ms The range for columns B and C is -1.0 to +3.0 ms Correlation coefficients are indicated at many of the peaks. Throughout this paper, three peaks of the AEPs labeled a, b, and c in this and subsequent figures are discussed. Polarity in these bipolar EPs has little meaning, but positivity is considered upward in all figures for the sake of discussion. In all NCCF and latency graphs, positivity is upward.

TABLE 1

REFERENCE WAVES

WAVE	LATENCY RANGE (ms)	DESCRIPTION
A	3.00 to 6.80	Major portion of the EP.
B	3.00 to 4.48	Early diphasic, fast negative peak (a) followed by slower, larger amplitude positive peak (b).
C	4.25 to 5.27	Middle-latency, slow, negative, monophasic peak (c).
D	5.04 to 6.80	Late, low-amplitude, fast activity.

TABLE 2

TEST WAVES

WAVE	TIME re. IMPACT, FIRST STIM (sec)	DESCRIPTION
1	-96	From control epoch, a subset of the baseline AEP.
2	+19	EP is undetectable, ripples or late slow wave may be EP activity.
3	+39	EP most likely present as indicated by NCCF analysis. In figure 1, two arrows indicate the most likely location of peaks b and c. Marked latency increase.
4	+86	EP clearly present; peaks b and c have altered shape; latency increase, but not as much as for wave 3.

row 1) indicated an excellent match between reference and test. The lowest peak correlation in row 1 was .91, and the greatest latency shift was 30 μs. Generally there are numerous of peaks in each NCCF. The highest peak (the one which indicated the best match) is referred to as the primary peak, and the others are referred to as secondary peaks. Note that if any of the secondary peaks were to achieve an amplitude comparable to that of the primary peak, erroneous results could have been obtained for peak correlation and latency shift. The more complex reference waves (A and D) yielded lower amplitude secondary peaks. In the post-impact data, there were smaller differences (figure 1, rows 2, 3, 4) between the primary and secondary peaks of the NCCFs, and selection of the correct primary peak was therefore less reliable.

In row 2 data, where the EP was essentially absent, the more complex reference waves (A and D) gave relatively low peak correlations, but the simpler reference waves (B and C) gave high peak correlations. The shapes of the row 2 NCCFs were substantially different than those from the pre-impact data (row 1). In rows 3 and 4, where the EP returned, the NCCFs began to approach the general appearance of the pre-impact NCCFs, and the more complex waves again gave high peak correlations. The position of the peaks in rows 3 and 4 clearly indicated an increase in latency. The average latency increase for all reference waves in row 4 was about 230 μs.

The Range of Shifts in Latency Indicated in NCCFs

The problem of secondary peaks can be ameliorated if the range of latency shifts allowed in the NCCFs is limited appropriately. There was no instance where a latency increase in these data was ever observed to exceed 1.0 ms in cases where the presence of the EP seemed relatively certain. It appeared reasonable, therefore, to eliminate shifts greater than +1.0 ms. Substantial latency decreases were not observed, and the NCCFs were truncated at -0.20 ms. The effect of truncation is shown in figure 2. This figure shows plots of the latency shifts and correlation coefficients at the maxima of the NCCFs. Time (in minutes) relative to the impact is represented on the abscissa. Plots are shown for two ranges of shift in latency: (A) -1.0 to +2.2 ms, and (B) -0.2 to +1.0 ms. The effect of truncation on the plots of shift in latency is apparent. The latency results were much less noisy with the narrower range. The effect of truncation on the correlation plots is less apparent but there was a small tendency toward lower correlations with the narrower range.

Plots From Various Reference Waves

Plots are shown in figure 3 (rows A-D) for the four reference waves of figure 1. The latency shift range of -0.2 to +1.0 ms was employed for all plots in this and subsequent figures. In the latency shift plots, the most complex reference wave (A) resulted in the smoothest plot. However, latency shift plots for the simpler reference waves provide important information. This may be seen by

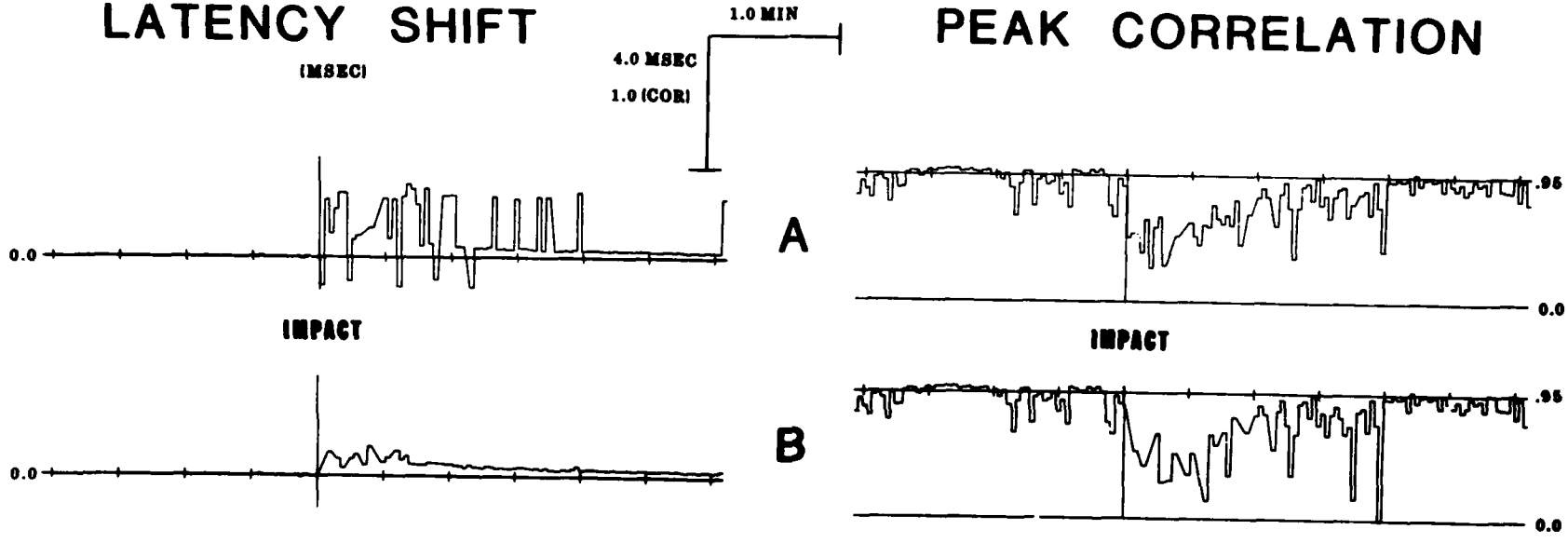

FIGURE 2

NCCF-derived latency shifts and peak correlations as a function of time relative to impact. The vertical axis indicates the time of impact. The purpose is to display the effects of truncation of the NCCFs. The latency shift range was -1.0 to +2.2 ms in row A, and -0.2 to +1.0 ms in row B (but the plot scales on rows A and B are the same). The reference (N=584) wave was wave A of figure 1. For each of the test waves, N is 8 to 10. In this and most subsequent figures, each graph has a ticked horizontal axis drawn through the pre-impact median, the value of which is given near the axis, and the peak correlation graphs generally have an additional horizontal axis drawn through zero correlation.

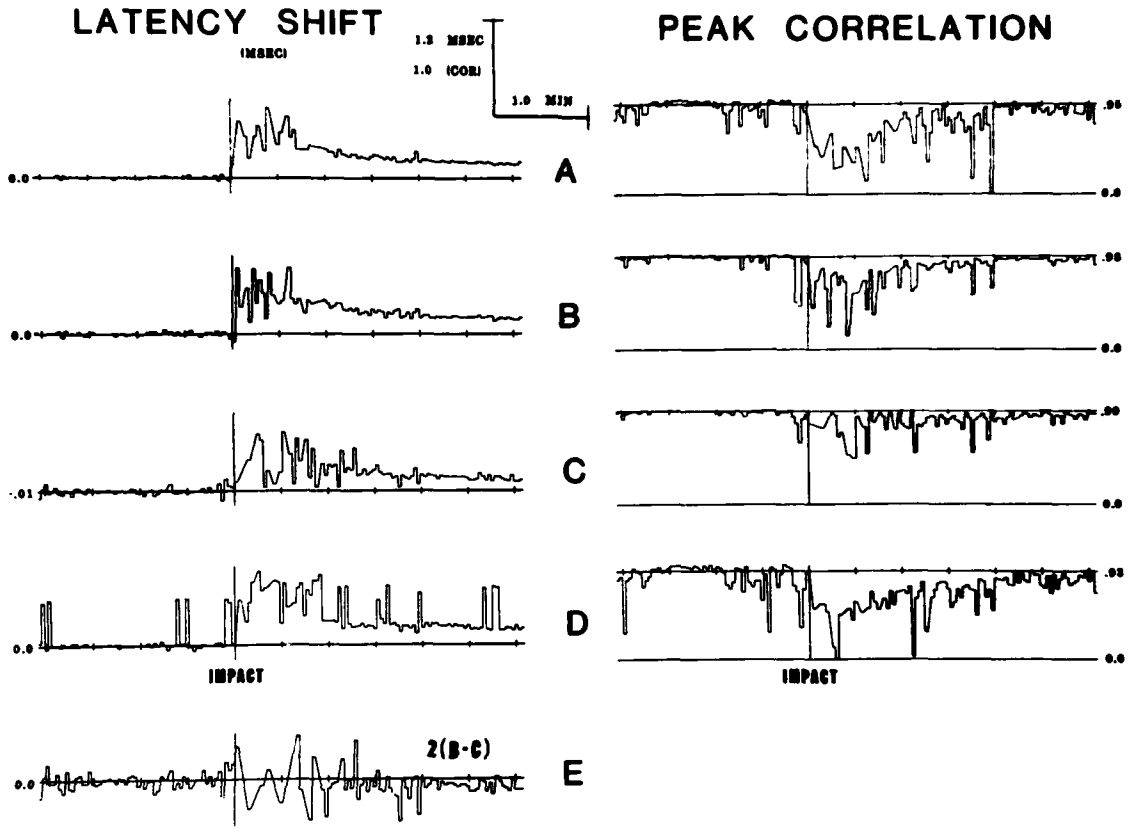

FIGURE 3

In rows A to D, latency shifts and peak correlations from four NCCFs using the four reference waves (N=584) of figure 1 are plotted as a function of time relative to impact. For each of the test waves, N is 8 to 10. The latency shift range was -0.2 to +1.0 ms Note that the vertical scale in these latency shift graphs is not the same as that of figure 2. Row E was obtained by subtracting the latency shifts in row C from those in row B, and is displayed with twice the vertical magnification of the other latency shift graphs in this figure.

comparing latency shift plots for reference wave B which represents the early part of the EP, with reference wave C which represents a later peak. During part of the post-impact period, the latency shift of the early part of the EP (B) was greater than that of the later part (C). This may be seen more clearly in figure 3, row E (note the vertical scale difference) in which a plot of the differences between the latency shifts in rows B and C is shown. The distribution of the differences between the post-impact portions of rows B and C was tested with the two-tailed Sign Test (using the normal approximation), and the null hypothesis was rejected at the 0.0001 significance level.

NCCF and Simple Peak Detection Compared with Respect to Latency

The results of the simple peak-detection algorithm are illustrated in figure 4 for comparison with the NCCF results. The latency results of figures 3 and 4 are to the same scale, and may be compared directly. Except at peak c, there was little difference between the two methods in the level of noise. However, the two methods of latency measurement gave substantially different results for the latency shifts in some cases. For example, the peak-detection plot for peak b (figure 4, row B) indicated a latency increase of 390 μs at 2.5 min. post-impact while the NCCF result for peaks a and b combined (figure 3, row B) indicated a latency increase of 210 μs at 2.5 min. post-impact.

Both procedures were run on unaveraged data in order to compare the two methods of latency measurement under more stringent conditions. The left column of figure 5 shows latency plots for peak-detection of three major peaks (labeled a, b, and c in figure 1). In the pre-impact period, the peak a latency (graph A) remained near the pre-impact median with little variability, while the pre-impact latencies for peaks b and c were more variable. During the first post-impact minute, however, the latency variability for all three peaks increased beyond levels that could be considered physiologically reasonable. This instability is due to failure in peak-detection. In the second post-impact minute, reasonable stability was again observed for peak a, while there was still little stability in the detection of peaks b and c. The NCCF using the complete AEP (graph D) was a little less stable than peak-detection of peak a (graph A). When the peak a was excluded from the reference wave (graph E), the NCCF result became slightly less stable, but was still more stable than than peak-detection of peaks b and c (graphs B and C).

Amplitude Measurement

Latency and waveshape were stable for averages of 10 EPs, and both peak-detection and NCCF methods worked well (figures 3 and 4). The peak-detection algorithm could therefore be used to study peak amplitude. Peak amplitudes were measured with reference to a pre-stimulus mean amplitude (figure 4, rows A, B, and C, corresponding to peaks a, b, and c of figure 1). Even in the control period under the best of circumstances, the EP peak amplitude was much more

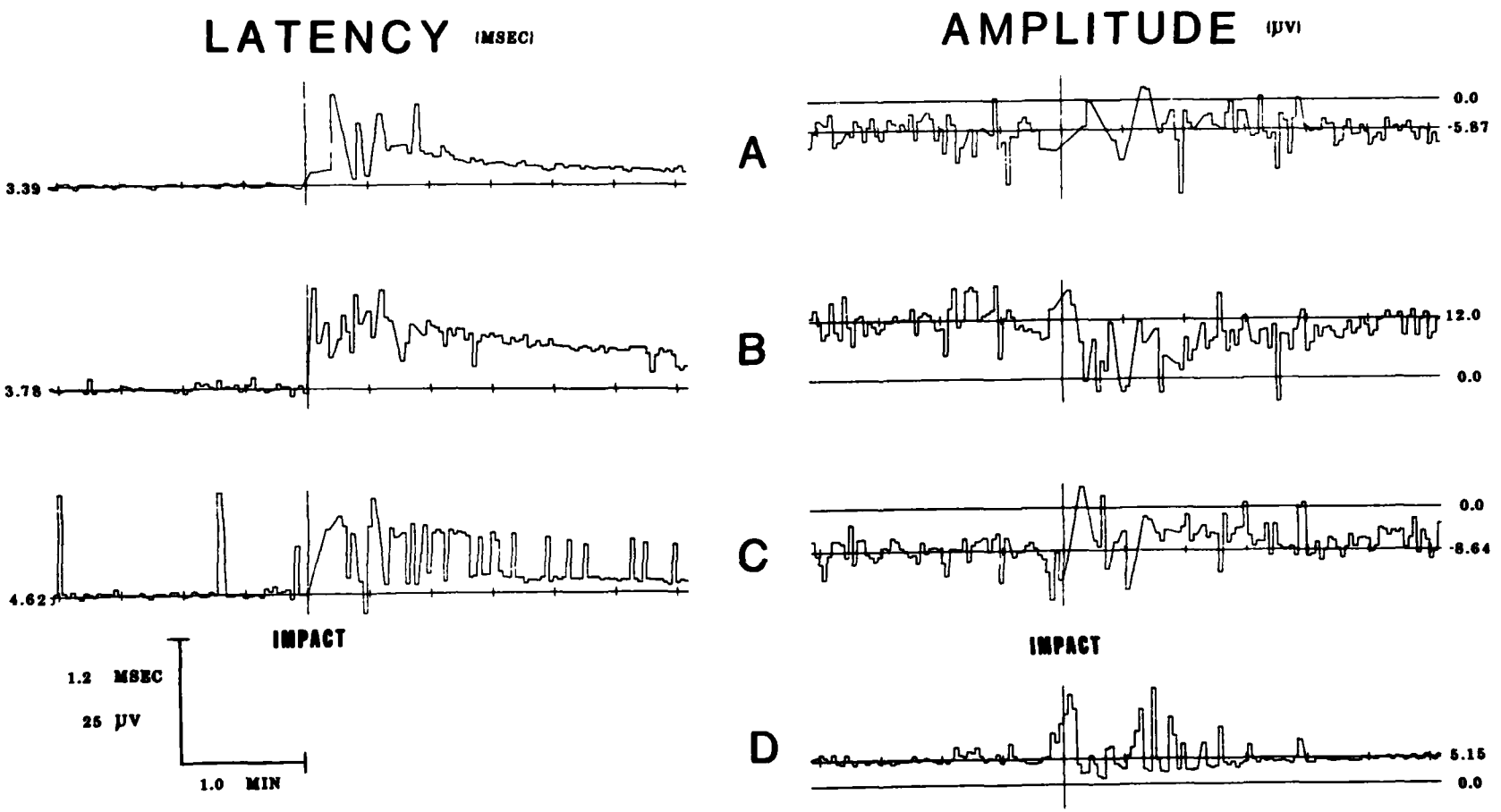

FIGURE 4

Rows A, B, and C are plots obtained using a simple peak-detecting algorithm to study peaks a, b and c of figure 1. For each row, a minimum (A and C) or a maximum (B) was sought in a 1.20 ms interval. The ranges scanned were: (A) 3.19 to 4.39, (B) 3.58 to 4.78, and (C) 4.42 to 5.62. The two columns display the latency, and the amplitude at the extrema. Row D is the overall amplitude in the interval 3.00 to 6.79 ms measured by estimating the RMS of the activity left in a selected interval after subtracting the mean amplitude in the interval.

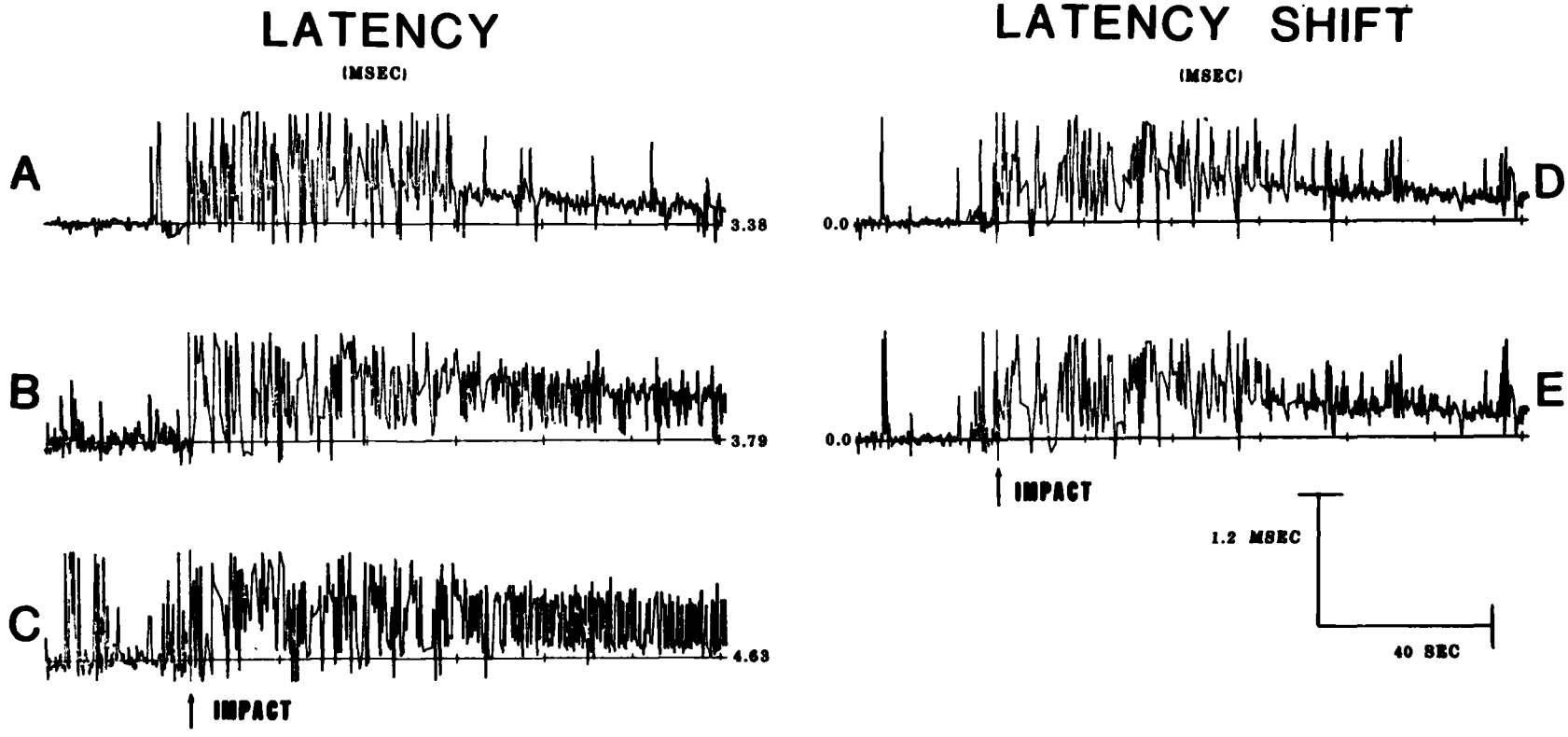

FIGURE 5

Graphs A, B, and C are the latency results of applying the simple peak-detecting algorithm to unaveraged EPs. The peaks and latency limits were the same as those in figure 4. Graphs D and E are the results of applying the NCCF analysis to the same unaveraged EPs. In D, the reference wave (N=150) was essentially the entire baseline AEP from the pre-impact time range displayed in this figure. The latency limits were 3.00 to 6.80 ms, and this reference wave is comparable to wave A of figure. 1. In E, the lower latency limit was increased to exclude the early, stable, negative peak measured in row A, leaving latency limits of 3.56 to 6.80 ms. The data analysed for this figure ranged from about 30 sec pre-impact to about 120 sec post-impact, and the horizontal scale is not comparable to that in previous figures.

variable than the peak latency measurement, and both NCCF measurements. The stability of the latency data in the control period indicate that this amplitude variability was a physiological effect and not a computation problem.

The results of RMS amplitude measurement are also shown in figure 4 (row D). The selected latency epoch included most of the AEP, and provided a shape-independent measure of overall amplitude of the AEP. The RMS amplitude measurement was less variable than the three peak amplitude measurements.

Use of Several Plots to Study Detailed Shape Changes at a Peak

There were impact-induced changes in the details of the shapes at peaks b and c which persisted for at least several minutes. In this section it is shown how several plots (figures 6 and 7) can be used in combination to study the details of such shape changes. Peak c was chosen for the example. AEPs with N from 40 to 50 were used in these two figures.

In figure 6, NCCF results for approximately 2 min. of pre-impact and 20 min. of post-impact data are shown. In row A of figure 6, the reference wave was the entire EP (3.00 to 6.80 ms, shown in figure 1). This reference wave supplied a reliable measure of overall latency shift of the entire AEP. In row B, a reference wave encompassing only peak c was used (4.25 to 5.27 ms, see figures 1 and 7). The latency shift stability resulting from this reference selection was comparable to that in row A. This suggested that the maximum correlation in row B was a reliable indication of shape behaviour at the peak. In contrast, when a somewhat narrower reference wave was used at the peak as shown in row C (4.46 to 5.18 ms, see figure 7) there resulted a bi-stable behaviour which suggested that there was a measurement problem with this reference wave. It thus appeared that the row 2 reference wave was just wide enough to provide stable NCCF results.

The nature of the instability that develops when the reference wave is too narrow can be determined from figure 7. Peak c appeared as if peaks from two waves were nearly superposed, resulting in a double peak, or sometimes a single peak and an inflection. When this complex peak was used for a reference wave, the resulting NCCF also tended to have a double peak or an inflection. The first peak (primary) of the NCCF corresponded to a correct match between reference and test waves, while the second (secondary) peak of the NCCF corresponded to a match of the first peak of the reference wave with the second peak of the test wave. This secondary peak became more prominent as the reference wave was made narrower, ultimately resulting bi-stable behaviour. These considerations support the conclusion that row B of figure 6 was indeed a reliable measure of shape change at the peak. It may be concluded that the shape at the peak was changed at impact, and essentially did not recover its pre-impact state over the 20 minutes displayed. Furthermore, it is noted that soon after impact, there was an especially drastic change at this peak which recovered to a more moderate change in under two

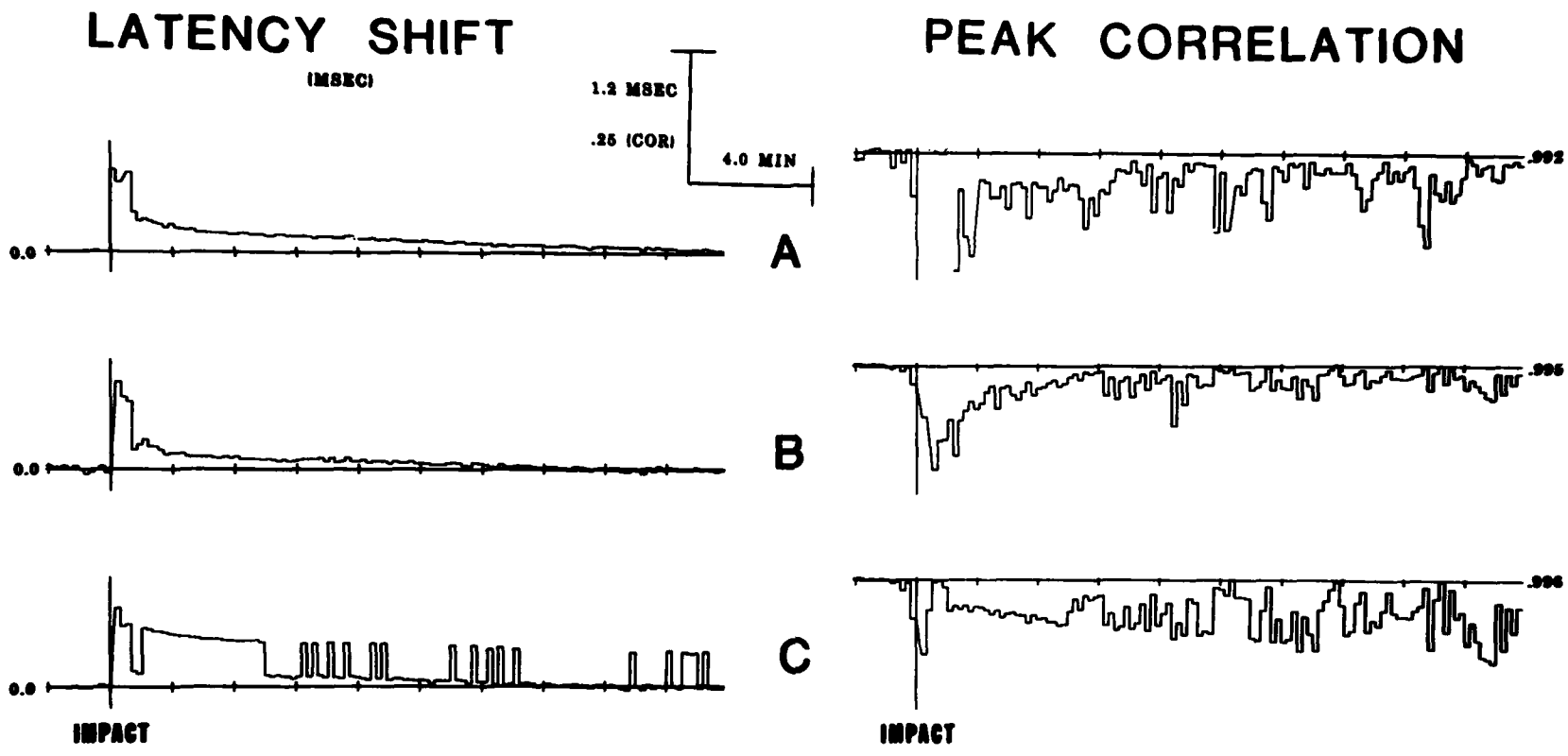

FIGURE 6

Application of the NCCF to the study of the details of the shape change of peak c (figure 1) is illustrated in this figure and figure 7. All graphs are the result of application of the NCCF procedure to data ranging from about 2 min. pre-impact to 20 min. post-impact. There are three choices of the latency range for the reference waves (N=584): (A) 3.00 to 6.80 ms, (B) 4.25 to 5.27 ms, and (C) 4.46 to 5.18 ms. For each of the test waves, N was 40 to 50. Row A provides a reliable measure of the overall latency shift. The latency shift stability in row B compares well with that in row A indicating that the correlation in row B is a good measure of the shape at peak c. The latency shift stability in row C differs markedly from that in row A, suggesting that the correlation in row C does not represent shape behaviour at the peak.

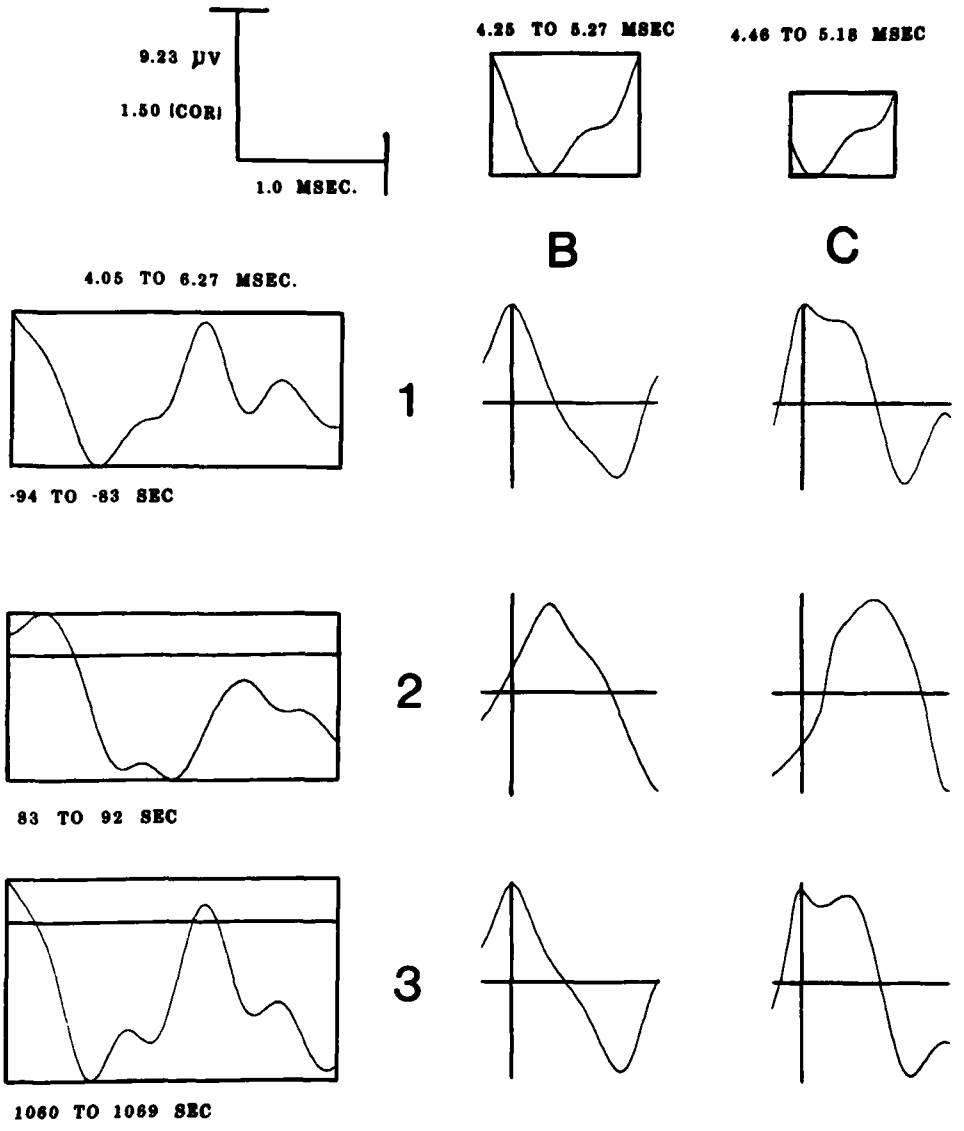

FIGURE 7

The six NCCFs obtained by applying two reference waves to three test waves are shown in matrix form. The two reference waves (B and C) are shown in the row at the top of the figure, and were used in rows B and C of figure 6. The reference waves are part of peak c of figure 1. The three test waves (1-3, N=49 or 50) are shown in the column at the left. Times (in ms) above the reference waves are the selected latency limits determining the reference waves. Times (in sec) below the test waves are the stimulus time limits (relative to impact) for the AEPs constituting the test waves. The latency range of the portion of the test waves displayed is 4.05 to 6.27 ms. All of the reference waves are taken from the same baseline pre-impact average (N=584). Latency shift range for each of the NCCFs is -0.2 to +1.0 ms.

minutes. These last findings are elaborated in the following section.

Polyexponential Regression

Three of the six graphs in figure 6 were subjected to polyexponential regression. They were: the overall latency shift, the peak c latency shift, and the peak maximum correlation. The other graphs in figure 6 were considered too noisy to provide meaningful results with polyexponential regression. The results are given in table 3 and figure 8, where they are designated A_L, B_L, and B_C respectively. In each of the graphs processed, a small number (not more than 4) of outlying points were arbitrarily dropped before the regression analysis. The peak c latency shift was adequately described by a single exponential decay term with a time constant of 7.3 min. The peak c maximum correlation required two exponential terms. One was a decay term with a time constant of 1.4 min., and the other was an exponential growth term with a time constant of 340 min. Since 340 min. is 17 times the duration of the data analysed, the longer term was interpreted as a constant asymptote for the shorter term, representing a permanent displacement from control values. The overall latency shift required two exponential decay terms with time constants of 10 min. and 35 sec. In each of the graphs analysed, some decrease in mean square error could be obtained by using three exponential terms, but the three term results were not considered meaningful.

DISCUSSION

The NCCF technique for quantification of EP data was examined and has a number of advantages. In most cases, the parameters are easy to set. There are four parameters, two specifying the portion of the baseline AEP to be used as the reference wave, and two specifying the limits of the latency shifts. Generally, the results are insensitive to small changes in these parameters. This allows effective preliminary analysis where the nature and latency of the EP is known only approximately. On the other hand, under certain predictable conditions, the choice of parameters can be quite critical. The detailed analysis of the shape at a peak c is a case in point.

The next advantage is that the resolution of the measurement can be easily traded against the sensitivity. Where the signal-to-noise ratio is high, narrow reference waves can be used to provide information about the waveshapes and latency shifts of various portions of the EP. Where the signal-to-noise ratio is low, wide reference waves can be used to increase detection reliability, resulting in measures of overall latency shift.

Another advantage of the NCCF method can be seen by comparing NCCF to peak-detection on peak b (figures 3 and 4). The peak-detection plot for peak b (figure 4, row B) indicates a strong and persistent latency increase after impact (390 μs at 2.5 min. post-impact). However, figure 1 shows that the shape at peak b

Overall Latency Shift, Reference: 3.00 to 6.80 ms A_L

# exp (MSEx10^5)		amp	time	amp	time	amp	time
1	co	0.29	-9.1				
(23.9)	se	0.0053	0.24				
* 2	co	0.25	-10.	0.42	-0.58		
(9.76)	se	0.0053	0.28	0.10	0.092		
3	co	0.49	-7.1	-1.2	-2.4	1.2	-1.7
(6.64)	se	0.11	0.69	0.067	0.35	0.061	0.15

Peak c Latency Shift, Reference: 4.25 to 5.23 ms B_L

# exp (MSEx10^5)		amp	time	amp	time	amp	time
* 1	co	0.25	-7.3				
(46.4)	se	0.0091	0.35				
2	co	0.10	-7.3	0.15	-7.3		
(46.4)	se	0.0046	0.27	0.0046	0.41		
3	co	0.13	-7.9	0.15	-7.9	0.84	-0.42
(43.0)	se	1.1	6815.	1.0	7980.	1.8	0.34

Peak c Maximum Correlation, Reference: 4.25 to 5.23 ms B_C

# exp (MSEx10^5)		amp	time	amp	time	amp	time
1	co	0.080	-10.				
(46.2)	se	0.0073	1.3				
* 2	co	0.025	+350.	0.20	-1.4		
(25.3)	se	0.0060	2000.	0.032	0.240		
3	co	5.2×10^{-7}	+1.9	0.034	-36.	0.21	-1.2
(24.8)	se	8.1×10^{-6}	2.8	0.013	54.	0.040	0.31

TABLE 3

The results of polyexponential regression of three of the six graphs in figure 6: (1) overall latency shift (A_L), (2) peak c latency shift (B_L), and (3) peak c maximum correlation (B_C). Graphic results appear in figure 8. For each of the three graphs, regression was run for one, two, and three term equations. The number of terms is given as # exp and below this is MSEx10^5, the mean square error multiplied by 10^5 (after subtracting the regression curve). For each term, amp is the exponential amplitude in appropriate units, and time is the time coefficient in minutes. A negative time coefficient indicates exponential decay while a positive time cofficient indicates exponential growth. For latency shifts, the amplitude units are milliseconds, and for peak correlations the amplitude units are correlation. The regression coefficients are in rows marked co, and the corresponding estimated standard errors are immediately below in rows marked se. An asterisk (*) marks the most meaningful set of coefficients for each of the three graphs fitted. In all cases, the pre-impact median was taken as zero for the regression analyses and, where the immediate effect of impact was a decrease in a measure, the exponential curves were inverted. Thus for the maximum correlation, a positive amplitude and a negative time coefficient indicate an initial decrease of the maximum correlation followed by a decay toward the high pre-impact value.

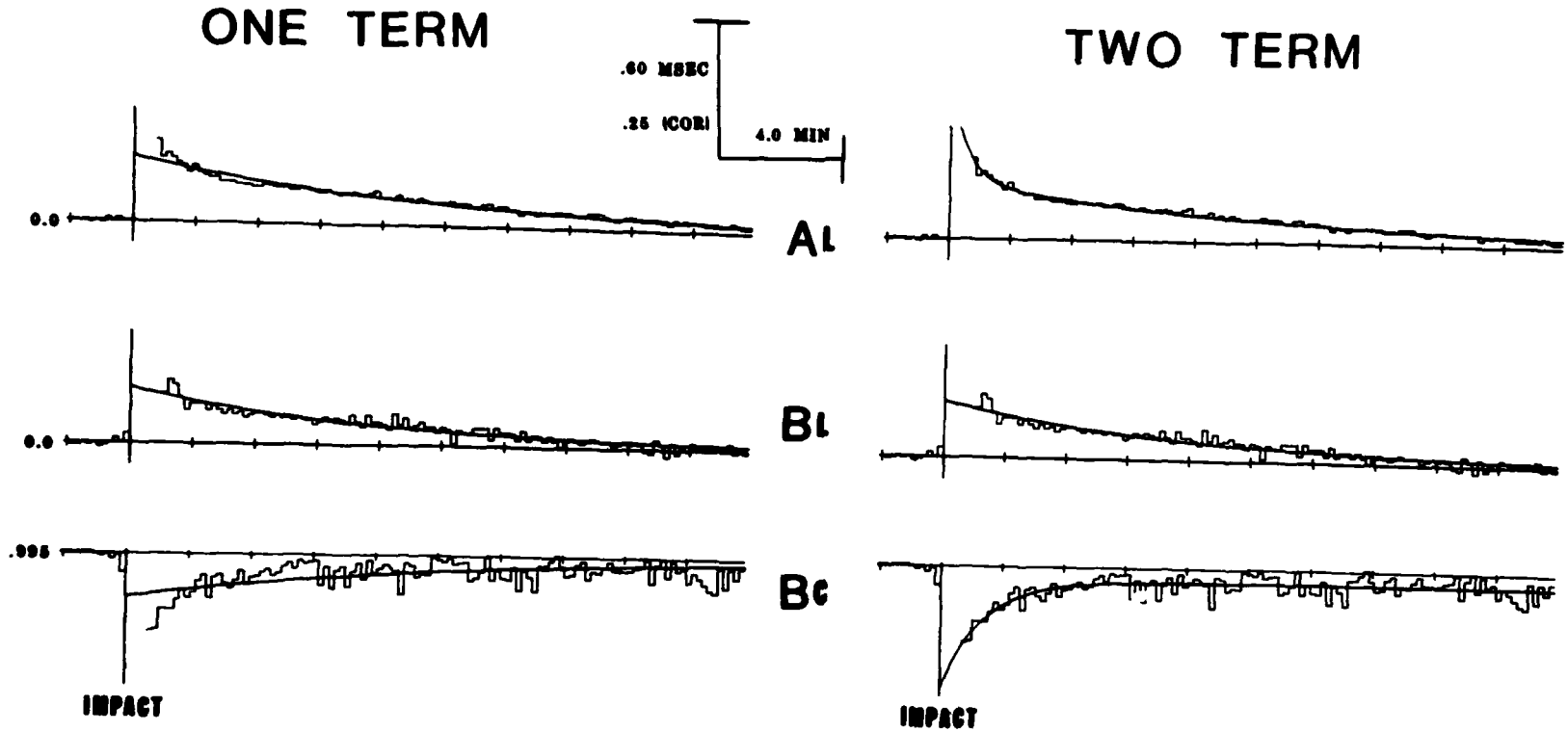

FIGURE 8

The results of polyexponential regression with one and two term polyexponential equations are shown on three of the graphs in figure 6: (A_L) overall latency shift, (B_L) peak c latency shift, and (B_C) peak c maximum correlation. Corresponding numerical data are given in table 3. Before regression, no more than four outlying points were dropped from each graph. Latency limits of the reference waves (N=584) were 3.00 to 6.80 ms for A_L, and 4.25 to 5.27 ms for B_L and B_C. The most meaningful fits appear to occur with one term for B_L and with two terms for A_L and B_C. For the test waves, N=40 to 50.

changed after impact in a way that would clearly affect the peak latency measurement, but would have little effect of NCCF latency shift measurement. The corresponding NCCF result (figure 3, row B) also shows a persistent latency increase, but of considerably smaller magnitude (210 μs at 2.5 min. post-impact). In data such as these, latency shift can be interpreted in terms of changes in conduction velocity, and the difference between the two types of measures could be of considerable consequence.

Finally, waveshape is difficult to define quantitatively in a concise way. One solution is to consider two EPs to be of the same shape by definition if the correlation coefficient between them is exactly unity, for some physiologically reasonable time shift between them. The NCCF may then be used to quantify the difference in shape between two waves. Measurement of waveshape is sensitive to a wide variety of changes that would be difficult to quantify with peak-detecting procedures, and would require taylored procedures for quantification. However, other procedures will generally be required to characterize the nature of changes detected with waveshape changes. The detailed results for peak c in figures 6 and 7 illustrate this.

In previous work (Weiss and Berger, 1978) waveshape comparisons were made using Pearson's correlation coefficient without allowing latency shift. The problems this would entail are evident in a comparison between the correlation coefficients at the peak with those at zero latency shift in figure 1 (especially rows 2, 3 and 4). In these data the two correlation coefficients differ drastically so that failure to allow latency shift seriously confounds shape change and latency shift. This has important implications in regard to use of factor analytic procedures for waveform analysis of data such as these. A number of authors have reported such work (Glaser and Ruchkin, 1978; Squires, et al., 1977). A property of the models underlying these procedures is that the EP is a linear combination of a small number of elementary waveforms. The linearity of the model implies that latency shift of these elementary waveforms is not permitted, especially when the degree of latency shift is continuous. (If latency shift is permitted in the model, at least one elementary waveform is required for each theoretically possible latency value.) The extent to which small latency shifts can become a problem for these linear factor analytic models is indicated approximately by the extent to which zero latency shift correlation differs from the peak correlation of the NCCF, as in figure 1. It is immediately apparent that in the post-impact data, application of such linear models would be inappropriate, especially in view of the apparently continuous latency changes seen in figures 3 and 6. The possibility remains that if the data were first corrected to remove the latency shift, factor analysis might be used. A procedure of this kind is used in the Woody filter (Woody, 1967).

The application of polyexponential regression to the present data was motivated by assuming a model in which impact produces a unidirectional effect that decays to the pre-impact baseline. This is equivalent to the assumption that the exponential amplitudes are positive and that the time coefficients are negative. In practice,

application of least squares sometimes results in coefficients with the wrong sign. In some cases, this presents little problem for interpretation. For example, the long, positive time coefficient for the two-term fit to the peak c maximum correlation could easily be the result of an asymptote that deviates from pre-impact data. On the other hand, the three-term result for the overall latency shift (table 3) presents a more difficult problem. In this case, there were two important changes in going from a two-term to a three-term fit. First, the short time coefficient (-.58 min.) disappeared and was replaced by two considerably longer time coefficients (-1.7 and -2.5 min.). Second, a negative amplitude appeared for one of these time coefficients. Examination of magnified residual graphs (not shown) revealed that the combination of these two terms (one with negative amplitude) was fitting a low level oscillation in the post-impact data. It is tentatively assumed that the oscillation was not related to the impact, and this three-term fit is considered inappropriate.

More generally, it has been found that the results of the polyexponential least-squares fit are quite sensitive to the starting values. For example, using the starting values supplied by CSTRIP, the two-term fit to the peak c latency shift merely duplicates the time coefficient of the one-term fit with no improvement in mean square deviation. However, by hand selecting the starting values, it is possible to obtain a faster decaying term that improves the fit of the first few points with consequent decrease in the mean square deviation. (This term did appear with CSTRIP starting values for the three-term fit of this graph.) Also, by appropriate selection of starting values, it is possible to fit a low level oscillation in the peak c latency shift with three terms, as was the case for the overall latency shift. The essence of the matter is that the polyexponential function can provide a number of very different good fits to a data set containing a moderate amount of noise. Selection among these fits must be guided by criteria other than strict adherence to the least-squares principle.

These difficulties notwithstanding, the polyexponential regression analysis is an effective technique for data such as these. The following conclusions concerning the time course of the EP changes summarized in table 3 and figure 8 appear warranted. There is clearly a double exponential decay in the overall latency shift. The time course of the peak c latency shift may be described with a single exponential decay term. This time constant was 73 percent of the slow time constant for the overall latency shift, and it is not clear whether the difference between these two slow time constants is meaningful. The peak c maximum correlation did not return to baseline in the time interval studied but there was a partial decay immediately after impact (-1.4 min.). This time constant is 2.4 times the fast time constant for overall latency shift and it appears that these two fast time constants represent different phenomena. A tentative interpretation of the shape changes indicated by the maximum correlation at peak c is that there were two nearly overlapping waves that were altered differently by impact.

As a final comment, it should be noted that the sample rate (100

kHz.) was quite high in view of the spectral content of the amplified signal. The gain was -3 dB at 1.5 kHz. and -15 dB at 3.0 kHz. In data filtered in this way, reliable latency shifts as low as 40 μs have been measured. If, in fact, the sampling rate is excessive in view of the information content of the signal, it would be expected that comparable results could be obtained using lower sampling rates and appropriate analytic techniques. Interpolation procedures have been applied to data sampled at lower rates yielding essentially the same results as those obtained at the high sampling rate.

CONCLUSIONS

The normalized cross-correlation function (NCCF) is an effective tool in the analysis of time dependent evoked potential data. By adjusting its four parameters (two to specify the portion of the baseline AEP used as the reference wave, and two to specify the portion of the test waves to be scanned), diverse aspects of the EP data can be quantified. Polyexponential regression, appropriately applied, was also useful in characterizing the present data. The NCCF provides measurements of shifts in latency and changes in waveshape. The NCCF should not be used in isolation, but in combination with other techniques that will provide measurements of amplitude, absolute latency, and additional information concerning changes in waveshape that are detected. In the present work, pre-impact baseline data were used to generate the reference waves. Other choices of reference data may be suitable in various experimental environments.

REFERENCES

Glaser, E.M. and Ruchkin, D.S. (1976), Principles of Neurobiological Signal Analysis, Academic Press, New York.

Metzler, C.M., Elfring, G.L. and McEwen, A.J. (1976), A Users Manual for NONLIN and Associated Programs, The Upjohn Co., Kalamazoo, Michigan.

Sedman, A.J. and Wagner, J.G. (1976), CSTRIP, a Fortran IV Computer Program for Obtaining Initial Polyexponential Parameter Estimates, Journal of Pharmaceutical Sciences, 65:1006-1010.

Squires, K.C. and Donchin, E. (1976), Beyond Averaging: The Use of Discriminent Functions to Recognize Event Related Potentials Elicited by Single Auditory Stimuli, Electroencephalography and Clinical Neurophysiology, 41:449-459.

Squires, K.S., Donchin, E., Herning, H.I. and McCarthy, G. (1977), On the Influence of Task Relevance and Stimulus Probability on Event-Related-Potential Components, Electroencephalography and Clinical Neurophysiology, 42:1-14.

Thomas, D.J., Robbins, D.H., Eppinger, R.H., King, A.I. and Hubbard, R.P. (1974), Guidelines for the Comparison of Human and Human Analogue Biomechanical Data, First Annual Report of an Ad-Hoc Committee, Ann Arbor, Michigan, December 6.

Thomas, D.J., Robbins, D.H., Eppinger, R.H., King, A.I., Hubbard, R.P. and Reynolds, H.M. (1975), Guidelines for the Comparison of Human and Human Analogue Biomechanical Data, Second Annual Report of an Ad-Hoc Committee, San Diego, California, November 19.

Walsh, P.R., Larson, S.J., Sances, A., Ewing, C.L., Thomas, D.J., Weiss, M.S., Berger, M., Myklebust, J. and Cusick, J.F. (1978), Experimental Methods for Evaluating Spinal Cord Injury During Impact Acceleration, Electrothereputic Sleep and Electroanesthesia, Vol. V, F.M. Wageneder and R.H. Germann, Eds., Universitat Graz, pp. 435-443.

Weiss, M.S., Berger, M.D. (1978), The Effect of Impact Acceleration on the Electrical Activity of the Brain, AGARD Conference Proceedings No.253, pp. A20-1 to A20-9.

Woody, C.D. (1967), Characterization of an Adaptive Filter for the Analysis of Variable Latency Neuroelectric Signals, Medical and Biological Engineering 5:539-553.